Letter

Truly relativistic gravity mediated entanglement protocol using superpositions of rotational energies

Gerard Higgins,[1,2,*] Andrea Di Biagio,[1,3,†] and Marios Christodoulou[1,‡]

[1]*Institute for Quantum Optics and Quantum Information (IQOQI), Austrian Academy of Sciences, A-1090 Vienna, Austria*

[2]*Department of Microtechnology and Nanoscience (MC2), Chalmers University of Technology, SE-412 96 Gothenburg, Sweden*

[3]*Basic Research Community for Physics e.V., Mariannenstraße 89, Leipzig, Germany*

(Received 5 March 2024; accepted 5 November 2024; published 26 November 2024)

Experimental proposals for testing quantum gravity-induced entanglement of masses (QGEM) typically involve two interacting masses which are each in a spatial superposition state. Here, we propose instead a QGEM experiment with two particles which are each in a superposition of rotational states; this amounts to a superposition of mass through mass-energy equivalence. In sharp contrast to the typical protocols studied, our proposal is genuinely relativistic. It does not consider a quantum positional degree of freedom and but relies on the fact that rotational energy gravitates: the effect we consider disappears in the $c \to \infty$ limit. Furthermore, this approach would test a feature unique to gravity since it amounts to sourcing a spacetime in superposition due to a superposition of "charge."

DOI: 10.1103/PhysRevD.110.L101901

Introduction. Accessing empirically the regime in which quantum gravitational effects could take place is notoriously difficult. One way, claimed impossible by Dyson [1,2], would be to detect quantized radiation. Another avenue is to probe the gravitational field sourced by a quantum mass [3]. This idea has received much attention in recent years with the progress in quantum control over increasingly large masses [4–6], and well studied specific proposals for detecting quantum gravity-induced entanglement of masses (QGEM) that leverage quantum information concepts and trends in quantum technologies [7–9]. Simple calculations using a direct Newtonian interaction show that two masses, each prepared in a position-delocalized state, will become entangled via the gravitational interaction. Linearized gravity predicts this effect [10–12], while theories in which the gravitational interaction is mediated by a classical local field do not predict the generation of entanglement [13,14]. Thus, gravitationally mediated entanglement would be a signature of the nonclassical nature of gravity. This is also supported by quantum information theoretic arguments that classical systems cannot mediate the creation of entanglement [15–17]. While QGEM does not involve direct detection of gravitons, there is an interesting indirect connection between QGEM and quantized radiation within quantum field theory [18–21].

QGEM schemes are typically imagined in the Newtonian regime and concern sourcing the gravitational field with masses that are prepared so that their positional degree of freedom is in a quantum superposition. Here, instead, we study a relativistic QGEM scheme. Instead of considering spatial superposition states, we take two particles that are each in a superposition of states of *different mass*, by preparing each particle in a superposition of rotational energy states and relying on mass-energy equivalence. In this case, not only G and $\hbar$ are relevant but *also* c: the effect disappears in the $c \to \infty$ limit. This idea is conceptually similar to the thought experiment discussed in Ref. [22], where it is shown that two clocks will get entangled due to the fact that a clock generally involves transitions between different energy states, and in Ref. [23], where neutrinolike oscillations are considered. QGEM protocols using particles in spatial superposition states and in superpositions of mass states are schematically represented in Fig. 1.

Performing such an experiment would be a more important test than the usual QGEM protocols that operate in the Newtonian regime. The protocol we study here relies on the general relativistic effect whereby the gravitational field can be sourced by rotational energy. This effect does not take place in Newtonian gravity, where the source of the gravitational field is the mass density. Because the use

*Contact author: gerard.higgins@oeaw.ac.at
†Contact author: andrea.dibiagio@oeaw.ac.at
‡Contact author: marios.christodoulou@oeaw.ac.at

Published by the American Physical Society under the terms of the Creative Commons Attribution 4.0 International license. Further distribution of this work must maintain attribution to the author(s) and the published article's title, journal citation, and DOI. Funded by Bibsam.

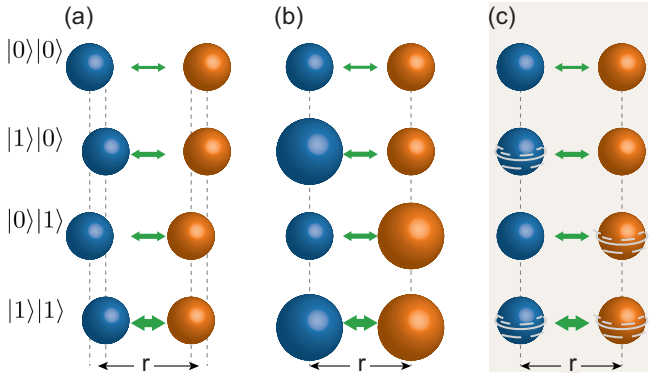


FIG. 1. QGEM protocols aim to witness whether the gravitational interaction between two masses can be in a superposition state. The typical approach considers (a) preparing each mass in a superposition of locations. Another possibility is to (b) prepare each particle in a superposition of mass states. Concretely, we show how this can be achieved by (c) preparing each particle in a superposition of rotational energies and exploiting the equivalence between mass and (rotational) energy.

of the mass energy results in a $1/c^4$ suppressing factor in the entangling phase, this test would be a more difficult experiment than detecting QGEM with spatial superposition states. However, this protocol would test a genuine interface between general relativity and quantum mechanics in the sense that there is no precise analog in electromagnetism as it would amount to considering a particle in a state superposition of electric charge which is excluded by superselection rules. We discuss the importance of this protocol in testing whether gravity can be treated as a classical variable in our concluding section.

Coming up with a realistic protocol to detect QGEM in mass superposition states is therefore not a trivial matter. This is the task for the current work. The protocol we discuss below goes some way in bringing this possibility to the realm of the feasible. Indeed, while we identify an operational "table top" parameter regime, a sober headed conclusion would be that the parameters we use are extremely ambitious and are not feasible for the foreseeable future.

We start with some general considerations of the difficulties in performing such an experiment. Then we consider a specific protocol for achieving a macroscopic superposition of rotational energies. We close with a discussion of our findings.

General considerations. The Hamiltonian for two particles interacting via gravity at a fixed separation r is $\hat{H} = -G\hat{M}_1\hat{M}_2/r$ where G is Newton's constant, and $\hat{M}_i$ is the mass operator acting on particle i [24]. We take each particle being initialized in an equal superposition of mass M and mass $M + \Delta M$, denoted as $|0\rangle$ and $|1\rangle$, $|\Psi(0)\rangle = \frac{1}{2}(|0\rangle + |1\rangle)(|0\rangle + |1\rangle)$. After time T the state of the system can be written as $|\Psi(T)\rangle = \frac{1}{2}(|00\rangle + |01\rangle + |10\rangle + e^{i\phi}|11\rangle)$, where $\phi = \frac{G}{\hbar}\frac{\Delta M^2 T}{r}$ (the calculation is described step by step in the Supplemental Material [25]). This two-qubit state is entangled if $\phi \neq 0$. The evolution of the two masses interacting via gravity can be interpreted as an entangling two-qubit controlled-phase gate, with ϕ the controlled phase shift [26]. The degree of entanglement of the state $|\Psi(T)\rangle$ can be quantified by the concurrence $|\sin 2\phi|$.

If the mass superposition ΔM is achieved by preparing each particle in a superposition of energy states, with energy difference E, the entangling phase is

$$\phi = \frac{G}{\hbar c^4}\frac{E^2 T}{r}. \tag{1}$$

Note the suppressing factor $1/c^4$ in the entangling phase which is due to the use of the mass-energy equivalence when considering a gravitating energy as we do here. If ϕ is small, then with N experimental repetitions, the statistical uncertainty in an estimate of ϕ is $\sim 1/\sqrt{N}$. To show that ϕ is nonzero, and that there is entanglement in the system, $N \sim 1/\phi^2$ experiment repetitions are needed.

A back-of-the-envelope estimate gives an initial idea of the challenging requirements: with evolution time $T = 1$ s, $N = 10^8$ repetitions (requiring a minimum total experiment time of ~ 3 years), and separation $r = 1$ μm, entanglement would become measurable if $\Delta M = 4 \times 10^{-18}$ kg $= 2 \times 10^9$ u and $E = 0.4$ J: a truly macroscopic energy superposition would be needed!

For example, it is unrealistic to consider the use of individual atoms or molecules in superpositions of electronic states, as these are separated by $E \sim 1$ eV $\approx 10^{-19}$ J. Similarly, if we assume that a large number of atoms or molecules are probed in parallel and long coherence times (record coherence times exceed 1 hour [27]), the phase remains unresolvable. The same applies for superpositions of nuclear states, since the fusion and fission processes typically involve energies $\sim 10^8$ eV $\sim 10^{-11}$ J.

A more realistic approach to creating superposition of mass energy with a view to testing QGEM is to consider two macroscopic solid massive rotors, each of which is set in a superposition of rotational energy states—and thus a superposition of masses—interacting via gravity.

A rotor with moment of inertia I in a superposition of rotating with angular velocity ω and angular velocity 0 is in a superposition of rotational energies with energy difference $E = \frac{1}{2}I\omega^2$. Substituting this energy difference into Eq. (1), the entangling phase which develops is $\phi = GI^2\omega^4 T/(4\hbar c^4 r)$. The general idea studied here can be thought of as investigating whether the quartic dependence of ϕ on the angular velocity ω can be used to offset the suppressing factor $1/c^4$. As we will see, there are several

other trade-offs that need to be considered in a realistic analysis.

For example, optically levitated nanoparticles [28] have indeed been spun up to very high GHz rotational frequencies using circularly polarized light [29,30]. However, this approach is not suitable due to the unwanted absorption of photons.

Instead, we consider two rotors, each with an embedded electric dipole moment and an embedded magnetic dipole moment, which can be controlled using electric fields and magnetic fields. We remark that using rotational degrees of freedom for gravitational entanglement has been proposed in [31], where a superposition of different static orientations of complex shapes leads to entanglement, while the more recent [32] proposes to entangle angular momentum degrees of freedom via the Lens-Thirring effect. For an introduction to the topic of spin-controlled rotors, see for instance the proposals in Refs. [33,34] and the experiments described in Refs. [35–37]. For a review of quantum phenomena that appear with rotating nanoparticles see Ref. [38].

Protocol. We consider two solid particles; each has a large magnetic dipole moment, as well as an embedded spin-1/2 particle corresponding to an electric dipole moment The idea is to use electric control of the relatively weak spin-1/2 electric dipole moment to prepare a superposition of orientations, then to use magnetic control of the relatively large magnetic dipole moment to spin up each particle. We describe the overall state of each particle in terms of the orientation of the spin-1/2 electric dipole moment $\{|0\rangle, |1\rangle\}$ and the orientation of the rest of the particle (which includes the embedded magnetic dipole moment) in terms of an angle θ and angular velocity ω, $|\theta, \omega\rangle$. We consider initiating each particle in state $|0\rangle \otimes |\theta = 0, \omega = 0\rangle$ and then applying the following steps:

(1) Prepare each spin-1/2 electric dipole moment in a superposition of orientations. After this step, each particle is in state $\frac{1}{\sqrt{2}}(|0\rangle + |1\rangle) \otimes |\theta = 0, \omega = 0\rangle$.
(2) Apply an electric field, to cause each particle to rotate to a superposition of orientations. This step lasts for time T_2. This results in the large embedded magnetic dipole moment having a superposition of orientations. After this step, each particle is in state $\frac{1}{\sqrt{2}}(|0\rangle \otimes |\theta = -\theta_0, \omega \approx 0\rangle + |1\rangle \otimes |\theta = \theta_0, \omega \approx 0\rangle)$.
(3) Apply an alternating magnetic field, to spin up each particle. The field is orientated along $-\theta_0$, so it effects a torque on only the $|1\rangle$ component of the superposition, and not on the $|0\rangle$ component. This step lasts for time T_3. After this step, each particle is in state $\frac{1}{\sqrt{2}}(|0\rangle \otimes |\theta = -\theta_0, \omega \approx 0\rangle + |1\rangle \otimes |\theta(t), \omega = \omega_{\max}\rangle)$.
(4) Allow the two particles to interact via gravity for time T_4.
(5) Reverse step (3).
(6) Reverse step (2).
(7) Measure.

Let us describe some of the steps in more detail:

Step (2): If the electric dipole moment states are initiated along the $\pm\hat{x}$ directions, application of an electric field along the $\hat{y}$ direction will cause a torque about the $\pm\hat{z}$ direction. This torque will have magnitude $p\mathcal{E}$, where $\mathcal{E}$ is the magnitude of the electric field. By the end of step (2) each component will be reorientated by an angle $\theta_0 \approx p\mathcal{E}T_2^2/(2I)$, where T_2 is the duration of this step and I is the particle's moment of inertia.

Step (3): A magnetic field then applies a torque on the $|1\rangle$ component and not on the $|0\rangle$ component. This is achieved by applying the field parallel with the orientation of the magnetic dipole moment of the $|0\rangle$ component. Figure 2 illustrates how the field can be alternated as the particle rotates to ensure that the torque is always about $\hat{z}$, and that only the $|1\rangle$ component is spun up.

With a magnetic field with strength B acting on the magnetic dipole moment m the maximum torque is $\tau_{\max} = mB$ (note that m refers to a magnetic moment and not a mass). The average torque during step (3) is approximately $\frac{2}{\pi}\tau_{\max}$ [cf. Fig. 2(e)]. The angular momentum of the $|1\rangle$ component will evolve to $I\omega_{\max} = \frac{2}{\pi}\tau_{\max}T_3 = \frac{2}{\pi}mBT_3$. To a good approximation, the angular velocity of the $|1\rangle$ component will increase linearly up to $\omega_{\max}$ during step (3), remain constant during step (4), then decrease linearly during step (5), as shown in Fig. 2(d).

The evolution of the angular velocity during step (3) depends on the separation between the orientations $2\theta_0$ at the end of step (2). The evolution will proceed fastest if $2\theta_0 = \pi/2$; this case is represented in Fig. 2. The more general cause, for lower values of θ_0, is described in the Supplemental Material [25].

In the next section, we will consider different effects which place limits on the protocol. Parameter regimes allowed by these effects are indicated in Fig. 3(a). We consider using two solid spheres. The main parameters are the sphere radii R, maximum angular velocity $\omega_{\max}$, and the duration of each step (we optimistically consider 10^3 s). We also consider particles of density 2.3×10^4 kg m^{-3}, which is the highest atmospheric pressure density of any element (osmium).

Operational limitations. We now consider three limitations and how to overcome them: the smallness of the entangling phase, centrifugal deformation, and spinning up without decoherence.

Entangling phase: The entangling phase ϕ that will develop over steps (2)–(4) is $\phi = \frac{G}{4\hbar c^4}\frac{I^2}{r}\int \omega(t)^4 dt \approx \frac{G}{4\hbar c^4}\frac{I^2\omega_{\max}^4}{r}(\frac{2T_3}{5} + T_4)$. We aim for phase $\phi > 10^{-3}$, to avoid

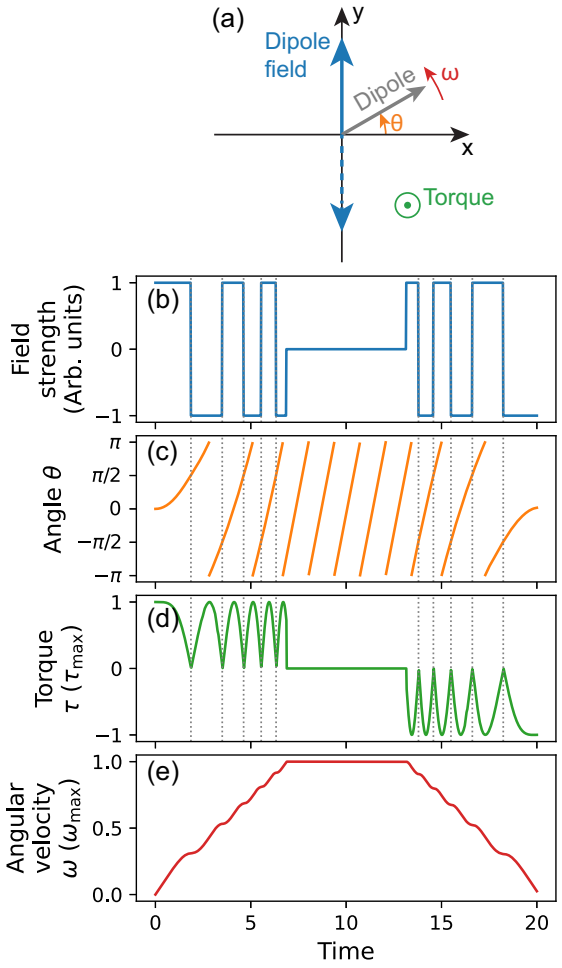


FIG. 2. A dipole field can be used to spin-up a dipole moment. (a) The dipole moment in the $x-y$ plane has polar angle θ. When $\pi/2 < \theta < 3\pi/2$ a field along $-\hat{y}$ is applied, otherwise a field along $\hat{y}$ is applied. This ensures the torque is always about $\hat{z}$. The process can be reversed. The subplots show, as a function of time, (b) the orientation of the applied field, (c) the dipole moments orientation, (d) the applied torque and (e) the dipole moments angular velocity.

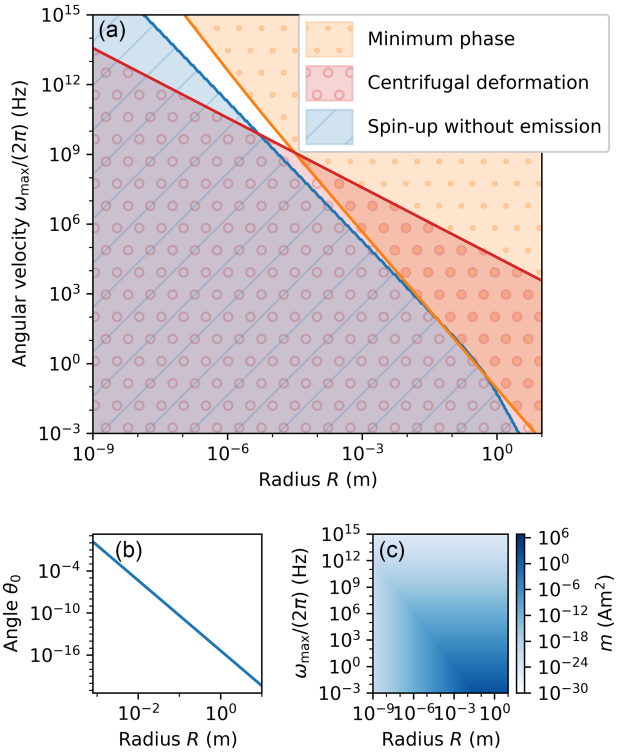


FIG. 3. (a) The shaded regions represent parameter regimes which satisfy the different requirements we consider. The shaded regions overlap for particles with radii around 0.1 m radius and angular velocities around $2\pi \times 1$ Hz, indicating the scheme may be viable for these parameters. (b) It becomes more difficult to prepare superpositions of orientations (separated by angle θ_0) during step (2) as the particle size and the moment of inertia is increased. (c) The magnetic dipole moment m is limited by the particle volume and remanence magnetization for small particles, and by the requirement that photons are not emitted for fast-spinning particles. These figures consider using two solid spheres.

requiring too many experimental repetitions for the phase to be resolved. Furthermore, very small values of ϕ would be difficult to measure reliably due to systematic uncertainties. This criterion is satisfied in the upper right region of Fig. 3(a) (orange dotted area), for higher values of $\omega_{\max}$ and higher particle radii R.

Centrifugal deformation: Fast spinning objects can irreversibly deform due to centrifugal forces. This happens when the tangential speed becomes comparable with the speed of sound in the material, introducing distinguishability between the spinning and nonspinning branches (components $|1\rangle$ and $|0\rangle$ respectively), thus causing decoherence. This is avoided in the lower left region of Fig. 3(a) (red region with open circles), for lower values of $\omega_{\max}$ and lower particle radii R. For the speed of sound in the particles, we use the highest physically allowed value of 3.7×10^4 m s^{-1} [39].

Spin-up without radiation emission: The third limitation we consider is somewhat more involved than the two introduced so far. It deals with whether it is possible to spin up the particle to $\omega_{\max}$ while avoiding decoherence caused by radiation.

With this in mind, first we need to consider the size of the superposition of orientations θ_0 achieved after step (2). The electric field strength we can consider applying during step (2) is $\mathcal{E} \approx 10^{10}$ Vm^{-1}, since matter is ionized in higher electric field strengths. We consider having control over electric dipole moments $p = 10^3$D; dipole moments of this magnitude were prepared in superposition states using laser light and microwave radiation in Ref. [40]. This gives a maximum torque $p\mathcal{E} \approx 10^{-17}$Nm during step (2). Figure 3(b) shows how the angle θ_0 that can be achieved decreases as the particle's moment of inertia is increased.

Then, whether or not the particle of radius R can be spun up to $\omega_{\max}$ depends on the magnitude of the embedded magnetic moment m, the strength of the applied magnetic field B, as well as on the size of the angular superposition θ_0 prepared during step (2).

Limits on the magnetic moment m are represented in Fig. 3(b). If the particles are small, m will be restricted by the particle volume V and the remanence magnetization M_{r} to $m = M_{\mathrm{r}}V$. We consider the high magnetization of neodymium $M_{\mathrm{r}} = 1.4$ T. If the particles spin with high angular velocities, m will be limited by the need to avoid emission of radiation, which we explain next.

The rotating magnetic dipole moment may emit electromagnetic radiation. If the rotating component of the superposition (state $|1\rangle$) emits a photon, then states $|0\rangle$ and $|1\rangle$ will be distinguishable, and the coherence between them will be lost. And so, the scheme requires there to be a low probability of photon emission.

The probability of emitting one or more photons is given by the overlap between the vacuum and the coherent state of the electromagnetic field sourced by the spinning branch, which is $e^{-\langle n\rangle}$, where $\langle n\rangle$ is the expectation number of the emitted photons. A classical magnetic dipole moment rotating with angular velocity ω radiates photons of energy $\hbar\omega$. The power emitted is given by $P = \omega^4 m^2/(6\pi\epsilon_0 c^5)$, and the rate of photon emission is $\dot{n} = \omega^3 m^2/(6\pi\epsilon_0\hbar c^5)$ and so, during steps (3)–(5), the expectation number of emitted photons is $\langle n\rangle = \omega_{\max}^3 m^2/(6\pi\epsilon_0\hbar c^5)(\frac{T_3}{3} + T_4)$. We limit m by requiring $\langle n\rangle < 1$. This limit impacts m in Fig. 3(c) if $\omega_{\max}$ is relatively high.

Then, the parameter regime which allows the particles with radii R and magnetic moment m to be spun up to $\omega_{\max}$ is indicated by the parameter regime with the blue striped lines in Fig. 3(a). This region is in the lower left part of the figure, since it is easier to spin up smaller particles with smaller moments of inertia to smaller angular velocities. Here we considered using a magnetic field with strength $B = 100$ T (this is around twice the record field strength that has been achieved in continuous operation [41,42]).

Overcoming the limitations: It appears to be possible to satisfy these three requirements for particles around $R \sim 0.1$ m and angular velocities $\omega_{\max} \sim 2\pi \times 1$ Hz, since the three shaded regions in Fig. 3(a) overlap around these parameters.

The overlap of the shaded regions improves if longer durations are allowed; however, the timescales we consider (10^3 s) are already extremely ambitious, since the experiment will be affected by other sources of decoherence [43,44]. These include blackbody radiation [45], collisions with background gas particles [45,46], and surface interactions between the rotors [47]. Achieving quantum coherence times around 10^3 s for solid particles with radii around 0.1 m is far, far beyond the current state of the art. Low temperatures and low background gas pressures many orders of magnitude beyond the current state of the art would be needed to mitigate these decoherence mechanisms.

As well as the parameters described so far, we considered a separation $r = 2R + r_{\min}$ between the spheres, where the minimum separation $r_{\min} = 10$ μm. While lower separations allow for stronger gravitational interactions, electric and magnetic interactions between the particles will need to be shielded. The value of $r_{\min}$ is chosen to allow for the possibility of an electromagnetic shield between the rotors.

Additional effects that arise due to trapping the rotors [48] are outside the scope of this work. A space-based experiment [49] could avoid the need for trapping, but this would raise other technical challenges.

One can consider different avenues for relaxing the experimental requirements. By reducing the separation between the masses, stronger gravitational interactions can be achieved. And so using two disc-shaped particles should enable larger operational parameter regimes than using two spheres, as we show in the Supplemental Material [25].

Conclusion. We have studied the possibility of using superposition of masses to detect entanglement mediation through gravity. In contrast to the typical QGEM proposals, this protocol is not described by Newtonian gravity. The superposition of mass is achieved through the use of superposition of rotational states and making use of the equivalence of rotational energy with mass. This setup for detecting mediated entanglement is also unique to gravity as the electromagnetic analog would involve a superposition of charge. Entanglement arises because rotational energy gravitates in general relativity, an effect that does not take place in Newtonian gravity (the effect disappears if we take $c \to \infty$).

The importance of detecting gravity mediated entanglement has been extensively discussed in the literature. The seminal papers [7,8] (see also [15,17]) presented no-go theorems stating that detection of gravity mediated entanglement that implies that, in any *local* theory, gravity must be mediated by a nonclassical system. These arguments are generalizations to postquantum theories of the well-known fact that local operations and classical communications cannot increase entanglement [16]. However, it is crucial to note that these theorems assume locality at the level of *subsystems*, which is a distinct notion from spacetime locality. While the latter is a well-established notion of locality in field theory, the subsystem notion of locality is on much weaker grounds, as one can have relativistically local theories with or without subsystem-local interactions [50–52].

A much less ambiguous way to state why these experiments are important is via the standard hypothesis testing route [53]: some theories predict the effect and some do not, and performing the experiment will allow us to distinguish between them.

Within linearized quantum gravity, the detection of mediated entanglement may be said to evidence that the gravitational field can be set in a quantum superposition of diffeomorphically inequivalent configurations [10,54,55].

Our protocol admits a similar interpretation as the usual QGEM protocol, with the main difference of going one step beyond the Newtonian limit of linearized quantum gravity, by witnessing the genuinely relativistic effect of energy sourcing the gravitational field. The relativistic nature of this effect is manifested in the strong suppressing factor $1/c^4$ in the entangling phase [Eq. (1)].

Another interesting distinction between our proposal and the spatial superposition QGEM experiments is that the effect has no electromagnetic analog, as it is well known that it is not possible to create a superposition of electric charges.

Our scheme involves achieving superpositions of rotations using control over electric dipole moments and magnetic dipole moments. The scheme gives a small parameter regime which may be operational; see Fig. 3. In order to achieve a workable regime, we had to make quite ambitious choices of parameters. While further improvements to our scheme are conceivable that may relax these parameters, we expect them to remain ambitious with respect to the current state of the art. We conclude that while it is conceivable to realize the task at hand in a "table top" setup, it would present a formidable experimental challenge and require significant technological improvements.

Acknowledgments. We thank Benjamin Stickler, Corentin Gut, and Markus Aspelmeyer for fruitful discussions. G. H. acknowledges support from the Swedish Research Council (Grant No. 2020-00381). M. C. and A. D. B. acknowledge support of the Grant ID No. 61466 from the John Templeton Foundation, as part of the "Quantum Information Structure of Spacetime (QISS)" project ([56]). This research was funded in whole or in part by the Austrian Science Fund (FWF) [10.55776/esp525].

[1] F. Dyson, Is a graviton detectable?, Int. J. Mod. Phys. A **28**, 1330041 (2013).
[2] T. Rothman and S. Boughn, Can gravitons be detected?, Found. Phys. **36**, 1801 (2006).
[3] *The Role of Gravitation in Physics: Report from the 1957 Chapel Hill Conference*, edited by C. DeWitt-Morette and D. Rickles (Max-Planck-Gesellschaft zur Förderung der Wissenschaften, Berlin, 2011), 10.34663/9783945561294-00.
[4] M. Aspelmeyer, T. J. Kippenberg, and F. Marquardt, Cavity optomechanics, Rev. Mod. Phys. **86**, 1391 (2014).
[5] M. Aspelmeyer, When Zeh meets Feynman: How to avoid the appearance of a classical world in gravity experiments, in *From Quantum to Classical: Essays in Honour of H.-Dieter Zeh* (Springer International Publishing, Cham, 2022), 10.1007/978-3-030-88781-0_5.
[6] T. Weiss, M. Roda-Llordes, E. Torrontegui, M. Aspelmeyer, and O. Romero-Isart, Large quantum delocalization of a levitated nanoparticle using optimal control: Applications for force sensing and entangling via weak forces, Phys. Rev. Lett. **127**, 023601 (2021).
[7] S. Bose, A. Mazumdar, G. W. Morley, H. Ulbricht, M. Toroš, M. Paternostro, A. Geraci, P. Barker, M. S. Kim, and G. Milburn, A spin entanglement witness for quantum gravity, Phys. Rev. Lett. **119**, 240401 (2017).
[8] C. Marletto and V. Vedral, Gravitationally-induced entanglement between two massive particles is sufficient evidence of quantum effects in gravity, Phys. Rev. Lett. **119**, 240402 (2017).
[9] T. Krisnanda, G. Y. Tham, M. Paternostro, and T. Paterek, Observable quantum entanglement due to gravity, npj Quantum Inf. **6**, 12 (2020).
[10] M. Christodoulou, A. Di Biagio, M. Aspelmeyer, Č. Brukner, C. Rovelli, and R. Howl, Locally mediated entanglement through gravity from first principles, Phys. Rev. Lett. **130**, 100202 (2023).
[11] R. J. Marshman, A. Mazumdar, and S. Bose, Locality and entanglement in table-top testing of the quantum nature of linearized gravity, Phys. Rev. A **101**, 052110 (2020).
[12] S. Bose, A. Mazumdar, M. Schut, and M. Toroš, Mechanism for the quantum natured gravitons to entangle masses, Phys. Rev. D **105**, 106028. (2022).
[13] D. Wallace, Quantum gravity at low energies, arXiv:2112.12235.
[14] J. Oppenheim, A postquantum theory of classical gravity?, Phys. Rev. X **13**, 041040 (2023).
[15] T. D. Galley, F. Giacomini, and J. H. Selby, A no-go theorem on the nature of the gravitational field beyond quantum theory, Quantum **6**, 779 (2022).
[16] R. Horodecki, P. Horodecki, M. Horodecki, and K. Horodecki, Quantum entanglement, Rev. Mod. Phys. **81**, 865 (2009).
[17] C. Marletto and V. Vedral, Witnessing the quantumness of a system by observing only its classical features, npj Quantum Inf. **3**, 1 (2017).
[18] D. Carney, Newton, entanglement, and the graviton, Phys. Rev. D **105**, 024029 (2022).
[19] A. Mari, G. De Palma, and V. Giovannetti, Experiments testing macroscopic quantum superpositions must be slow, Sci. Rep. **6**, 22777 (2016).
[20] A. Belenchia, R. M. Wald, F. Giacomini, E. Castro-Ruiz, Č. Brukner, and M. Aspelmeyer, Quantum superposition of massive objects and the quantization of gravity, Phys. Rev. D **98**, 126009 (2018).

[21] D. L. Danielson, G. Satishchandran, and R. M. Wald, Gravitationally mediated entanglement: Newtonian field versus gravitons, Phys. Rev. D **105**, 086001 (2022).
[22] E. Castro Ruiz, F. Giacomini, and Č. Brukner, Entanglement of quantum clocks through gravity, Proc. Natl. Acad. Sci. U.S.A. **114**, E2303 (2017).
[23] C. Marletto, V. Vedral, and D. Deutsch, Quantum-gravity effects could in principle be witnessed in neutrino-like oscillations, New J. Phys. **20**, 083011 (2018).
[24] M. Zych, Quantum systems under gravitational time dilation, Ph.D. thesis, University of Vienna, 2017, Springer Theses.
[25] See Supplemental material at http://link.aps.org/supplemental/10.1103/PhysRevD.110.L101901 which includes information about the generation of entanglement between two particles which are initialized in mass-superposition states, the dynamics during step (3) of the protocol, and the feasibility of the scheme when disc-shaped particles are used.
[26] E. Polino, B. Polacchi, D. Poderini, I. Agresti, G. Carvacho, F. Sciarrino, A. D. Biagio, C. Rovelli, and M. Christodoulou, Photonic implementation of quantum gravity simulator, Adv. Photonics Nexus **3**, 036011 (2024).
[27] P. Wang, C.-Y. Luan, M. Qiao, M. Um, J. Zhang, Y. Wang, X. Yuan, M. Gu, J. Zhang, and K. Kim, Single ion qubit with estimated coherence time exceeding one hour, Nat. Commun. **12**, 233 (2021).
[28] S. Kuhn, A. Kosloff, B. A. Stickler, F. Patolsky, K. Hornberger, M. Arndt, and J. Millen, Full rotational control of levitated silicon nanorods, Optica **4**, 356 (2017).
[29] J. Ahn, Z. Xu, J. Bang, Y.-H. Deng, T. M. Hoang, Q. Han, R.-M. Ma, and T. Li, Optically levitated nanodumbbell torsion balance and GHz nanomechanical rotor, Phys. Rev. Lett. **121**, 033603 (2018).
[30] R. Reimann, M. Doderer, E. Hebestreit, R. Diehl, M. Frimmer, D. Windey, F. Tebbenjohanns, and L. Novotny, GHz rotation of an optically trapped nanoparticle in vacuum, Phys. Rev. Lett. **121**, 033602 (2018).
[31] J. S. Pedernales, F. Cosco, and M. B. Plenio, Decoherence-free rotational degrees of freedom for quantum applications, Phys. Rev. Lett. **125**, 090501 (2020).
[32] T. B. Lantaño, L. Petruzziello, S. F. Huelga, and M. B. Plenio, Low-energy test of quantum gravity via angular momentum entanglement, arXiv:2409.01364.
[33] C. C. Rusconi, M. Perdriat, G. Hétet, O. Romero-Isart, and B. A. Stickler, Spin-controlled quantum interference of levitated nanorotors, Phys. Rev. Lett. **129**, 093605 (2022).
[34] Y. Ma, M. S. Kim, and B. A. Stickler, Torque-free manipulation of nanoparticle rotations via embedded spins, Phys. Rev. B **104**, 134310 (2021).
[35] E. Urban, N. Glikin, S. Mouradian, K. Krimmel, B. Hemmerling, and H. Haeffner, Coherent control of the rotational degree of freedom of a two-ion Coulomb crystal, Phys. Rev. Lett. **123**, 133202 (2019).
[36] T. Delord, P. Huillery, L. Nicolas, and G. Hétet, Spin-cooling of the motion of a trapped diamond, Nature (London) **580**, 56 (2020).
[37] Y. Jin, K. Shen, P. Ju, X. Gao, C. Zu, A. J. Grine, and T. Li, Quantum control and fast rotation of levitated diamonds in high vacuum, Nat. Commun. **15**, 5063 (2024).
[38] B. A. Stickler, K. Hornberger, and M. S. Kim, Quantum rotations of nanoparticles, Nat. Rev. Phys. **3**, 589 (2021).
[39] K. Trachenko, B. Monserrat, C. J. Pickard, and V. V. Brazhkin, Speed of sound from fundamental physical constants, Sci. Adv. **6**, eabc8662 (2020).
[40] C. Zhang, F. Pokorny, W. Li, G. Higgins, A. Pöschl, I. Lesanovsky, and M. Hennrich, Submicrosecond entangling gate between trapped ions via Rydberg interaction, Nature (London) **580**, 345 (2020).
[41] J. Miller, The NHMFL 45-T hybrid magnet system: past, present, and future, IEEE Trans. Appl. Supercond. **13**, 1385 (2003).
[42] S. Hahn, K. Kim, K. Kim, X. Hu, T. Painter, I. Dixon, S. Kim, K. R. Bhattarai, S. Noguchi, J. Jaroszynski, and D. C. Larbalestier, 45.5-Tesla direct-current magnetic field generated with a high-temperature superconducting magnet, Nature (London) **570**, 496 (2019).
[43] C. Zhong and F. Robicheaux, Decoherence of rotational degrees of freedom, Phys. Rev. A **94**, 052109 (2016).
[44] B. A. Stickler, B. Schrinski, and K. Hornberger, Rotational friction and diffusion of quantum rotors, Phys. Rev. Lett. **121**, 040401 (2018).
[45] D. E. Chang, C. A. Regal, S. B. Papp, D. J. Wilson, J. Ye, O. Painter, H. J. Kimble, and P. Zoller, Cavity opto-mechanics using an optically levitated nanosphere, Proc. Natl. Acad. Sci. U.S.A. **107**, 1005 (2010).
[46] L. Martinetz, K. Hornberger, and B. A. Stickler, Gas-induced friction and diffusion of rigid rotors, Phys. Rev. E **97**, 052112 (2018).
[47] L. Martinetz, K. Hornberger, and B. A. Stickler, Surface-induced decoherence and heating of charged particles, PRX Quantum **3**, 030327 (2022).
[48] L. Martinetz, K. Hornberger, and B. A. Stickler, Electric trapping and circuit cooling of charged nanorotors, New J. Phys. **23**, 093001 (2021).
[49] R. Kaltenbaek *et al.*, MAQRO—BPS 2023 research campaign whitepaper, arXiv:2202.01535.
[50] A. Di Biagio, R. Howl, Č. Brukner, C. Rovelli, and M. Christodoulou, Relativistic locality can imply subsystem locality, arXiv:2305.05645.
[51] V. Fragkos, M. Kopp, and I. Pikovski, On inference of quantization from gravitationally induced entanglement, AVS Quantum Sci. **4**, 045601 (2023).
[52] M. Christodoulou, A. Di Biagio, R. Howl, and C. Rovelli, Gravity entanglement, quantum reference systems, degrees of freedom, Classical Quantum Gravity **40**, 047001 (2023).
[53] N. Huggett, N. Linnemann, and M. D. Schneider, *Quantum Gravity in a Laboratory?*, 1st ed. (Cambridge University Press, Cambridge, England, 2023), 10.1017/9781009327541.
[54] M. Christodoulou and C. Rovelli, On the possibility of laboratory evidence for quantum superposition of geometries, Phys. Lett. B **792**, 64 (2019).
[55] E. Martín-Martínez and T. R. Perche, What gravity mediated entanglement can really tell us about quantum gravity, Phys. Rev. D **108**, L101702 (2023).
[56] https://www.qiss.fr/